Journal of Applied Physics

RESEARCH ARTICLE | NOVEMBER 18 2013

Raman intensity profiles of zone-folded modes in SiC: Identification of stacking sequence of 10H-SiC

S. Nakashima; T. Tomita; N. Kuwahara; T. Mitani; M. Tomobe; S. Nishizawa; H. Okumura

J. Appl. Phys. 114, 193510 (2013)
https://doi.org/10.1063/1.4828996

Raman intensity profiles of zone-folded modes in SiC: Identification of stacking sequence of 10H-SiC

S. Nakashima,[1,a)] T. Tomita,[2] N. Kuwahara,[2] T. Mitani,[1] M. Tomobe,[1,3] S. Nishizawa,[1] and H. Okumura[1]

[1]*National Institute of Advanced Industrial Science and Technology, Advanced Power Electronics Research Center, Umezono 1-1-1, Central 2, Tsukuba, Ibaraki 305-8568, Japan*
[2]*Faculty of Engineering, The University of Tokushima, 2-1, Josanjima, Tokushima 770-8506, Japan*
[3]*Graduate School of Integrated Basic Sciences, Nihon University, 3-25-40 Setagaya, Tokyo 156-8550, Japan*

(Received 23 August 2013; accepted 14 October 2013; published online 18 November 2013)

Raman intensity profiles are measured for 10H-SiC crystals, for which various zone-folded phonon modes are observed. Raman intensity profiles are calculated based on a bond polarizability model assuming several stacking sequences for the 10H polytype using a linear chain model. Among several candidates for the stacking sequences, the 3322 stacking structure provides the best-fit profile for experimental spectral profiles. The hexagonality value of 0.4 predicted from the stacking sequence of this polytype is consistent with that derived from the frequency splitting between the experimental A_1 and E-type transverse optical modes. This fact is consistent with an empirical rule that the value of the reduced wavevector for the strongest folded transverse acoustic and optical modes are equal to the hexagonality of the polytype. In the present analysis of the Raman intensity profiles, the calculated intensity profiles for specified folded transverse optical modes are found to be relatively strong and strikingly dependent on force-field parameters in α-SiC that consists of the mixture of the cubic and hexagonal stacking structures. These force-field parameters can reproduce well the experimental Raman intensity profiles of various SiC polytypes including 10H-SiC. [http://dx.doi.org/10.1063/1.4828996]

I. INTRODUCTION

It is well known that SiC has a large number of polytypes with different stackings of Si-C double layers. All polytypes except for the 3C polytype belong to uniaxial crystals and are anisotropic in structural, optical, transport, and phonon properties. The crystal structures of SiC polytypes are determined through X-ray diffraction, electron microscope, and Raman scattering analyses. Raman intensity analysis is useful in identifying the stacking sequence of the Si-C double layers along the *c*-axis.[1–4] It also provides information on anisotropic phonon properties in a-SiC.[5,6]

SiC polytypes form natural superlattices whose periods are integral multiples of the 3C polytype-period. By zone folding of the higher-ordered polytypes, the phonon modes within the basic Brillouin zone and at the zone edge are folded back to the Γ point and can be observed in Raman spectra. The relative Raman intensity of the zone-folded modes yields information on the stacking structure of polytypes. Thus far, polytype structures of SiC have been examined using Raman intensity analysis for a number of long-period polytypes, 8H,[1] 15R,[1] 21R,[1] 27R,[2] 33R-SiC.[7] The structure of the long-period polytype of 132R-SiC was also determined from Raman intensity analysis.[8] The period of this polytype was inferred from the frequencies of the observed folding modes, with reference to the dispersion curves.[2] Raman intensity profiles were calculated for possible structure candidates and compared with the experimental Raman profile. Finally, a polytype structure corresponding to the best-fit Raman profile was chosen. The stacking structure estimated from this Raman analysis, being $[(33)_3(32)_2(33)_2 22]_3$, showed agreement with the structure obtained by a pseudo-reflection high-energy electron diffraction.[8]

Up to now, various numbers of SiC polytypes have been studied by X-ray diffraction and electron microscope analyses. The presence of 10H-polytype was first reported by Ramsdell and Kohn in 1951.[9] They pointed out that the space group of this polytype was C_{3v}^1 (C3 m1), being different form that of 4H and 6H. The report by Pandey and Krishnan[10] in 1975 stated that the stacking sequence of this polytype was 3322 in Zhdanov notation. Since then, however, the experimental structure analysis of this polytype has not been studied for a long time. It was pointed out by Inoue that possible hexagonal structures for polytypes with 10H-SiC layers are 82, 55, and 3322 in Zhdanov notation.[11] The stacking fault structures of 15R[$(32)_3$] were studied theoretically by Iwata *et al.* who suggested that there are several stacking faults including 3322.[12] Backes *et al.*[13] calculated the band-gap energy of 10H-SiC assuming that the stacking sequence of this polytype is 55. The total energy differences between various polytypes were calculated by Limpijumnong and Lambrecht,[14] where they regarded 10H-SiC as 55. More recently, Kobayashi and Komatsu calculated electronic and lattice properties for various long period polytypes.[15] In their calculation, they dealt with various possible stacking structures of 10H-SiC. The presence of these theoretical studies suggests that experimental identification of the stacking sequence for this polytype is desirable.

[a)]nakashima-s@aist.go.jp

So far the intensity analysis of Raman spectral profiles based on the bond polarizability model has been applied to the structural identification of SiC polytypes[1,2,16] and of layer compounds.[17,18] The Raman polarizability is related to the arrangement of the bond Raman polarizabilities and atomic displacements which are obtained from lattice dynamical calculations. The Raman intensity profiles calculated previously[1,2] reproduced qualitatively the experimental Raman intensity profiles which enabled us to identify the stacking sequences of various SiC polytypes. In this lattice dynamical calculation, force constant parameters were chosen so that the calculated frequencies of phonons fit the measured frequencies. This approach enabled Raman intensity profiles to be calculated consistent with observation, but it did not always account for the measured intensity of folded modes, especially for weak folded modes. Therefore, more detailed study was required for analysis of the Raman intensity profiles in SiC.

In the present work, the Raman intensity profiles of 10H-SiC has been measured. It is found that a certain folded transverse optical band has relatively increased strength. A similar feature was also found for 27R-SiC crystal.[2] We have calculated Raman intensity profiles of the 10H-SiC and revealed that the calculated intensity of the folded modes in this polytype is sensitive to the force-field difference between the cubic and hexagonal environments. The present analysis shows that the distortion of the atomic displacement patterns derived from the force-field difference provides enhancement of Raman strength of the folded mode. The stacking sequence of the 10H-SiC is identified from a comparison between observed and calculated spectra.

II. THEORETICAL BACKGROUND

A. Raman intensity analysis

To date, several attempts have been made to explain the Raman intensity profiles in crystals. A widely used approach is based on "bond polarizability model," which was initiated by Wolkenstein[19] and Eliashevich and Wolkenstein,[20] and successfully applied to molecules by Long.[21] Raman polarizability tensors with respect to the phonon coordinates have been calculated for highly symmetric crystals by Tubino and Piseri,[22] Go *et al.*,[23] and Maradudin and Burstein.[24] The method of the Raman intensity analysis based on the bond polarizability concept have been developed by Nakashima *et al.* to interpret the Raman spectral profiles of the folded transverse optical (FTO) and folded transverse acoustic (FTA) modes in SiC polytypes, and succeeded for the structure identification of various SiC polytypes.[1,2,8] The Raman intensity of folded longitudinal optical (FLO) and folded longitudinal acoustic (FLA) modes in 4H-, 6H-, 15R-, and 21R-SiC were also analyzed based on the bond polarizability model.[3] A reasonable agreement between the experimental calculated intensity profiles was obtained.

The Raman scattering intensity is related to the bond Raman polarizabilities and relative displacement between neighboring Si and C atomic layers, and is given as[26]

$$I(\omega) = A\frac{n(\omega)+1}{\omega}|\Delta\alpha'(\omega)|^2 = A\frac{n(\omega)+1}{\omega}\left|\sum_n \alpha'(n)[u(n:\omega)-v(n:\omega)]\exp(iqz_n)\right|^2, \quad (1)$$

where $\alpha'(n)$ is a bond Raman polarizability, $u(n:\omega) - v(n:\omega)$ the relative displacement between the n-th neighboring Si-C layers, z_n the central position of the bond along the c-axis, $n(\omega)$ the Bose factor, and A a constant of proportionality. This equation indicates that the Raman intensity profile is closely related to the relative displacements of the neighboring Si-C bonds and the arrangement of the bond Raman polarizabilities.

For the FTA and FTO modes (E-type modes) in SiC, the bond tilted against the c-axis contributes to the Raman polarizability in Eq. (1), whereas there is no contribution from the bond parallel to the c-axis. The tilted bonds in SiC are divided into two groups. A plus sign is assigned to the group of bonds (a) α-B, β-C, and γ-A, and minus sign to the group of bonds (b) α-C, β-A, and γ-B or vice versa. Here, the Roman letters A, B, C, and Greek letters α, β, γ represent the positions of silicon and carbon atoms, respectively.[1]

B. Lattice dynamics

The displacement amplitudes of the atomic planes are obtained as solutions of the equation of motion

$$-M_j\ddot{u}_j = \sum_n D_{j,j+n}u_{j+n}, \quad (2)$$

where $D_{j,j+n}$ is the interplanar force constant between planes j and $j+n$. We assume traveling wave solutions of exponential form. We obtain the dispersion relations from the condition that Eq. (2) has nontrivial solutions

$$|\delta_{ij}M_j^2\omega^2 - D_{ij}(q)| = 0. \quad (3)$$

We shall consider a simple one-dimensional model of SiC crystals, as illustrated in Fig. 1, which displays the stacking of the Si-C planes along the [0001] direction for the 10H polytype. The stacking structure 3322 for this polytype is determined in the present work, together with the connecting forces. The 10H (3322) polytype contains four hexagonal and six cubic stackings in the unit cell. The interplanar forces up to the third-neighbor plane are taken into account. In this model, the nearest-neighbor plane forces K_{-1}^{cs}, K_{+1}^{cs}, and the third-neighbor plane force K_3^{cs} are taken to be independent of the stacking environment, whereas the second- and third-neighbor plane forces $K_2^{ss}(=K_1)$, K_2^{cc} $(=K_2)$, and K_{-3}^{cs} $(=K_3)$ depend on the stacking environment and these differ for the cubic and hexagonal environments. For the cubic configuration, we take $K_i + \Delta K_i$, whereas for the hexagonal configuration, we take $K_i - \Delta K_i$.

A set of force-field parameters are determined as follows. First, these are roughly determined so that for the 3C polytype the calculated phonon dispersion curve fits the experimental dispersion curve. Second, these are determined more precisely so that the calculated Raman intensity profiles for various

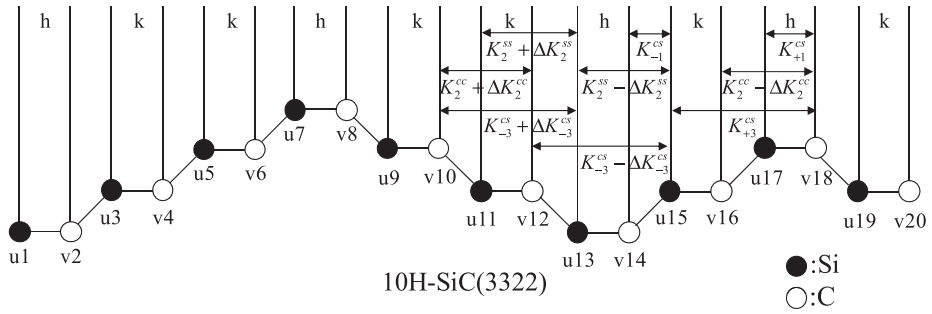

FIG. 1. Stacking structure and force field for 10H-SiC (3322); *h* and *k* represent the hexagonal and cubic stackings, respectively.

polytypes well reproduce the experimental profiles. The detailed procedure will be discussed in Sec. III C later on. The force-field parameters thus determined are listed in Table I. Instead of K_2^{ss}, K_2^{cc}, and K_{-3}^{cs}, we shall use the notation ΔK_1, ΔK_2, and ΔK_3, hereafter. The set of force constants listed in Table I can be used as universal parameters to calculate the Raman intensity profiles for various SiC polytypes.

C. Raman intensity profile in zinc-blende structure approximation

In assuming that the second- and third-neighbor force fields in α-SiC are equal for the hexagonal and cubic envelopments, we then are considering the zinc-blend structure approximation for α-SiC where we have

$$\Delta\alpha'(\omega) = [u(n:\omega) - v(n:\omega)]\sum_n \alpha'(n)\exp(iqz_n) = [u(\omega) - v(\omega)]S(q). \quad (4)$$

In this approximation, the displacement amplitudes of the Si and C planes are independent of their positions and

$$\begin{aligned} I(\omega) &= A\frac{n(\omega)+1}{\omega}|\Delta\alpha'(\omega)|^2 \\ &= A\frac{n(\omega)+1}{\omega}\left|\sum_m [u(m:\omega) - v(m:\omega)]\alpha'(m)\exp(iqz_m)\right|^2 \\ &= A\frac{n(\omega)+1}{\omega}|u(m:\omega) - v(m:\omega)||S(q)|^2 \\ &= A\frac{n(\omega)+1}{\omega}|u(m:\omega) - v(m:\omega)|c(q), \end{aligned} \quad (5)$$

$$c(q) = \sum_m c(n)\exp(-iqz_m), \quad c(n) = \sum_m \alpha'(n)\alpha'(n+m), \quad (6)$$

where z_m is the position of the m-th atom, and $\omega = \omega(q)$ the q-dependent frequency of the folded modes. Function $u(m:\omega)$-$v(m:\omega)$ is the relative displacement of the m-th neighboring Si-C atomic planes which are separated by (1/4)c for the folded mode of frequency ω.

III. EXPERIMENTAL

A. Sample preparation and Raman measurements

The 10H-SiC polytype samples used in this Raman measurement were Rely crystals, and the sample used was a 0.5-mm-thick flake of approximately 10 × 5 mm in size with the c(0001) face. The 10H-SiC (3322) structure belongs to the symmorphic space group of P3m1 (C_{3v}^1). The primitive unit cell contains 20 atoms, and the lattice modes at the Γ point are decomposed into

$$\Gamma_{tot} = 20\,A_1 + 20\,E.$$

The optical modes decompose into

$$\Gamma_{opt} = 19A_1 + 19E.$$

Raman scattering spectra have been measured in the backscattering geometry at room temperature using a double monochromater with focal length of 1 m. The 514.5-nm line of an Ar laser was used for the Raman measurement. An optical microscope with an objective lens of NA = 0.8 was used in the laser illumination of the sample and the collection of the scattered light. Raman scattering signals were detected using a liquid-nitrogen-cooled CCD detector.

B. Raman spectral profile of 10H-SiC

We measured Raman spectra of a 10H-SiC crystal in the backscattering geometry using the (0001)-face. Figure 2(a) shows a spectrum of the FTA phonon modes, and Fig. 2(b) shows FTO modes measured using the (0001) face. Because the folded mode in nH or 3nR polytypes corresponds to the phonon mode at q(x) = q(2 m/n),(0 ≤ 2 m ≤ n) in the basic zone of the 3C polytype, the FTA and FTO modes are expected to appear at q(2 m/10), (0 ≤ m ≤ 5) for the 10H polytype.

As shown in Figs. 2(a) and 2(b), the q(4/10)-folded mode at 785.5 cm^{-1} which has a reduced wavevector equal to the hexagonality of the 3322 structure (= 0.4) displays the maximum intensity for the FTA and FTO modes. Because the zone-folded modes correspond to the modes at certain

TABLE I. Force constant parameters used in the linear chain model shown in Fig. 1; values are in units of 10^4 dyne/cm.

K_{-1}^{CS}	K_{+1}^{CS}	K_2^{SS}	K_2^{CC}	K_{-3}^{CS}	K_{+3}^{CS}	$\Delta K_2^{SS}(=\Delta K_1)$	$\Delta K_2^{CC}(=\Delta K_2)$	$\Delta K_{-3}^{CS}(=\Delta K_3)$
27.3	5.38	0.493	0.211	−1.81	0.717	0.2	0.235	−0.16

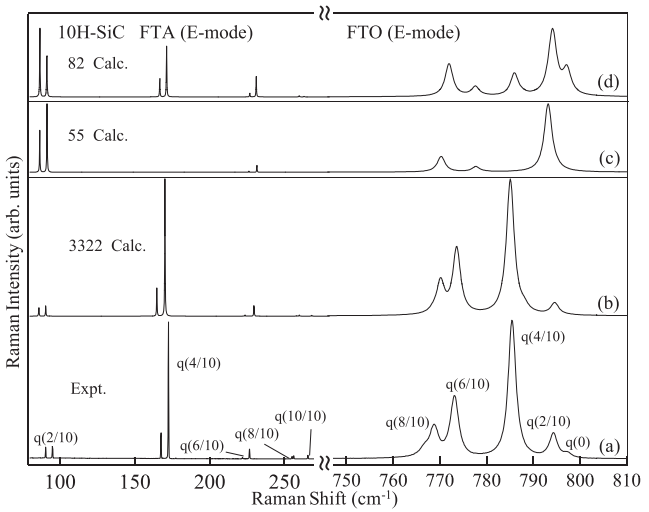

FIG. 2. (a) Whole Raman spectrum of 10H-SiC (3322) observed in the backscattering geometry using the *c*-face, (b) calculated Raman spectrum of the 3322 stacking structure, (c) calculated Raman spectrum of the 55 stacking structure, and (d) calculated spectrum of the 82 stacking structure.

q points, the phonon mode at q in the basic zone is denoted as the $q(x)$ mode hereafter, where $x = q/q_B$ is the reduced wavevector, $q_B = \pi/c$, and c is the unit cell length along the [111] direction of the 3C polytype (zinc blende).

As shown in Fig. 2(a), for the FTA modes, all the folded modes except the FTA(10/10) mode exhibit doublets. For the FTO modes, doublets are not observed because the bandwidth is large and the doublets are unresolved.

C. Comparison with observed and calculated spectra of 10H-SiC

We have calculated Raman intensity profiles of the stacking sequence 3322. The spectra calculated using Eqs. (1)–(6) are shown in Fig. 2(b), where the intensity is normalized by that of the $q(4/10)$ mode. The agreement between the observed (Fig. 2(a)) and calculated spectra (Fig. 2(b)) is quite satisfactory for the stacking sequence of 3322, though there are slight deviations in peak frequencies of the low-lying modes.

D. Comparison with calculated 55 and 82 spectra

Figures 2(c) and 2(d) show the calculated Raman intensity profiles of the 55 and 82 stacking structures, where ΔK_i is included in the force field. The calculated FTA and FTO spectral profiles for the 3322 sequence in Fig. 2(b) reproduce well the experimental profile of Fig. 2(a) and are quite different from the calculated spectral profiles of 55 and 82. This result suggests strongly that the real stacking structure of 10H-SiC is 3322.

E. Raman spectra of a-face

Raman spectra are also observed using the *a*-face of the 10H-SiC sample in the backscattering geometry (see Figs. 3(a) and 3(b)). In the transverse optical (TO) mode region in Fig. 3(a), the unfolded TO(A_1) and TO(E) modes appear at 785.3 and 797.4 cm^{-1}, respectively. The FLO modes with $q(2\,m/10)$ ($m = 1$, 2, 3, 4, and 5) are also observed. In

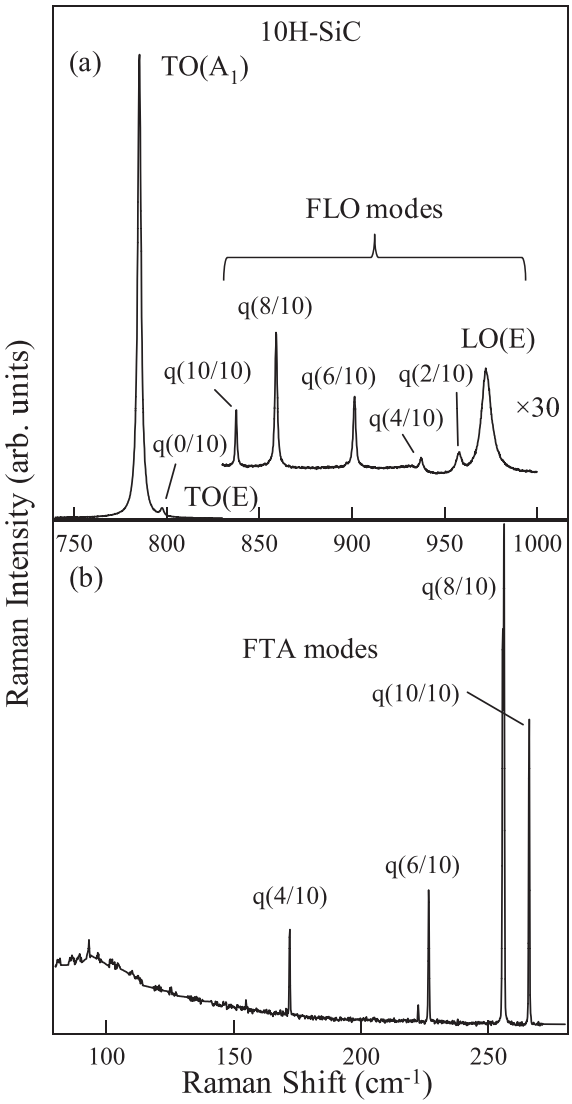

FIG. 3. Raman spectra of 10H-SiC(3322) observed with the *a*-face at backscattering geometry: (a) spectra of the optical phonon region, and (b) spectrum of acoustical phonon region.

the FTA mode region of Fig. 3(b), relatively strong FTA modes appear at $q/q_B = 4/10$, 6/10, 8/10, and 10/10. The experimental frequencies of the folded modes of 10H-SiC which are observed using the *c*- and *a*-faces are listed in Table II ((a) and (b)), respectively. Note that the frequencies of the FTA modes for the *a*-face measurement are slightly different from that for the *c*-face measurement and that the frequency splitting between the doublets for the *a*-face measurement is smaller than for the *c*-face measurement. This fact arises from the dispersion of the acoustic phonon branch in the *z*-direction. The splitting of the FTA doublet modes depends on the wavevector, q_z, of the phonon associated with the Raman process; q_z is different for the *c*- and *a*-face measurements. It was observed by Nakashima and Tahara that the frequency splitting of the FTA doublet varies with the wavelength of the excitation laser.[25]

F. The most intense Raman mode and hexagonality

As stated before, the Raman intensity profile of SiC polytype crystals depends on the stacking sequence. In a proposal

TABLE II. Raman frequencies of the folded modes for 10H-SiC measured using (a) *c*-face and (b) *a*-face in the backscattering geometry.

(a) c-face measurement					
		Frequency (cm^{-1})			
	$x = q/q_B$	FTA	FTO	FLA	FLO
10 H	0	—	796.9 (E)	—	965.4 (A_1)
	2/10	90.5, 95.1 (E)	794.3 (E)	168.7, 177.5 (A_1)	—
	4/10	167.5, 172.5 (E)	785.5 (E)	329.5, 337.8 (A_1)	—
	6/10	222.0, 226.6 (E)	773.1 (E)	466.4, 474.4 (A_1)	896.9, 901.6 (A_1)
	8/10	255.1, 256.2 (E)	768.8 (E)	568.8, 572.8 (A_1)	858.3, 860.0 (A_1)
	10/10	265.8 (E)	766.9 (E)	611.8 (A_1)	—
(b) a-face measurement					
		Frequency (cm^{-1})			
	$x = q/q_B$	FTA	TO, FTO	FLA	LO, FLO
10 H	0	—	797.4 (E), 785.3 (A_1)	—	972.6 (E)
	2/10	—	—	—	958.0 (E)
	4/10	172.0	—	—	937.2 (E)
	6/10	222.4, 226.5	—	467.9, 473.1	901.4 (E)
	8/10	255.7, 256.1	—	570.3	859.1 (E)
	10/10	265.9	—	611.8	837.6 (E)

by Nakashima *et al.*,[26] the reduced wavevector ($x = q/q_B$) of the strongest FTA and FTO modes is equal to the hexagonality of the SiC polytype. This empirical rule was confirmed by Raman intensity measurements for various polytypes.[26]

This rule predicts that for the 10H-SiC (3322) structure the folded modes with $q/q_B = 0.4$ has maximum intensity, which indeed is true for the FTO and FTA modes as shown in Fig. 2.

G. Phonon anisotropy and hexagonality

The crystal structures and phonon properties for the α-SiC polytypes are both anisotropic. This anisotropy produces the frequency splitting between TO phonon modes with E and A_1 symmetries.[5,6] Raman spectra of the $E(E_1)$- and A_1-type TO modes using the *a*-face were observed for various SiC polytypes.[6] It was found that the frequency splitting, $\Delta\omega = \omega(E) - \omega(A_1)$, is related linearly to the hexagonality, *h*, as shown in Fig. 4, with a constant of proportionality β of 29.6. The result for the 10H polytype structure lies on the $\Delta\omega$ vs *h* curve, indicating that the hexagonality of 10H-SiC is 0.4. This conclusion is consistent with the estimate derived from the stacking sequence of 3322.

IV. DISCUSSION

A. Raman intensity and force fields

As discussed in Sec. II, Raman spectral profiles of the FTO modes depend strongly on the force-field parameters. The calculated spectral profiles are especially sensitive to the difference of the forces between cubic and hexagonal environments ΔK_i. When we take the force fields in the two environments as being equal, these fields resemble those of the 3C polytype and the atomic displacement pattern is given by that for 3C. In this case, the Raman intensity enhancement arising from distorted atomic displacements decreases and there remains solely the contribution from the arrangement of the bond Raman polarizabilities.

To confirm that the force-field difference ΔK_i actually affects the Raman intensity profile, experimental Raman spectra of the FTO modes for the 15R, 6H, 27R, and 10H polytypes were plotted (see Fig. 5). The intensity of each folded mode calculated assuming that ΔK_i is zero is indicated by horizontal bars in this figure. The calculated Raman intensity of the FTO modes almost coincides with those observed when $\Delta K_i \neq 0$, namely, we use the force parameters listed in Table I, whereas the calculated peak intensity is reduced when we take $\Delta K_i = 0$, as seen in Fig. 5. For the

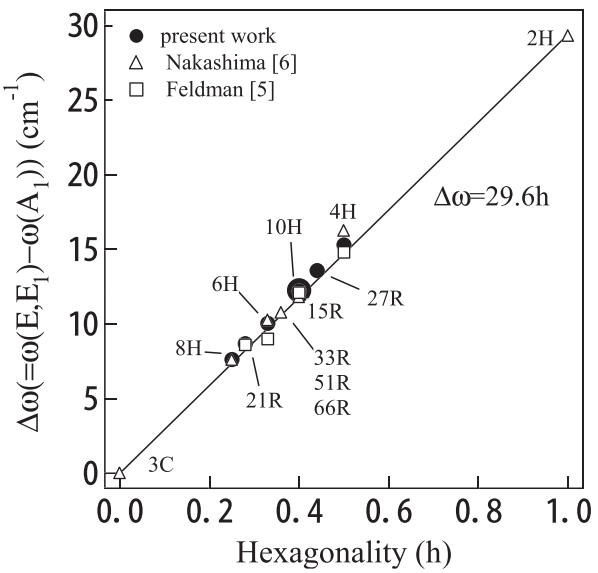

FIG. 4. The frequency splitting between E(TO) and A_1(TO) modes $\Delta\omega$ plotted against the hexagonality; these phonon modes are measured using the *a*-face.

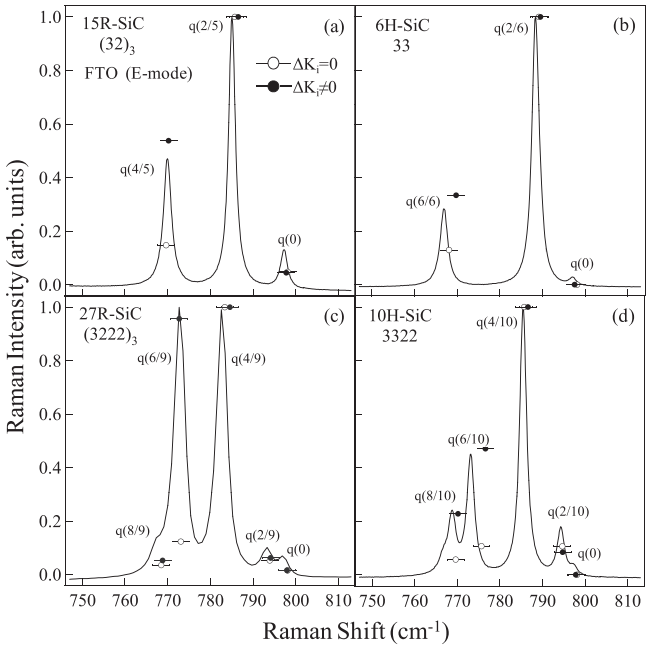

FIG. 5. Raman spectra of (a) 15H-, (b) 6H-, (c) 27R-, and (d) 10H-SiC observed in the backscattering geometry using the *c*-face. Raman intensity of the FTO modes, calculated assuming that $\Delta\omega = 0$, is shown by horizontal bars.

27R, the reduction of the calculated intensity for $\Delta K_i = 0$ is striking for the $q(6/9)$ mode, being 13% of the observed phonon mode.

B. Force field dependence of Raman intensity

We found that the calculated Raman intensity profiles of the FTO modes in 10H-SiC (3322) vary markedly by the introduction of the force-field difference between the hexagonal and cubic environments, ΔK_i. In Fig. 6, we present the calculated intensity of the $q(6/10)$ FTO mode relative to the $q(4/10)$ mode as a function of the force parameter ΔK_2. The intensity of the FTO modes depends also on the force

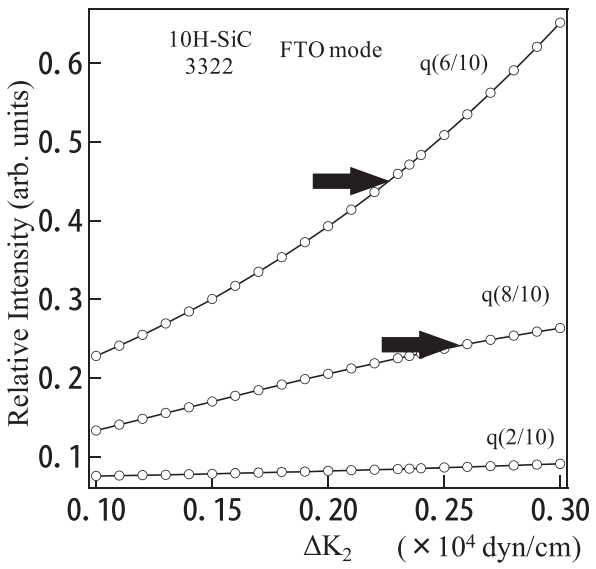

FIG. 6. Calculated relative Raman intensity of $q(6/10)$, $q(8/10)$, and $q(2/10)$ FTO modes as a function of ΔK_2. The intensity of each mode is normalized by the intensity of $q(4/10)$ mode; arrows mark experimental intensity data.

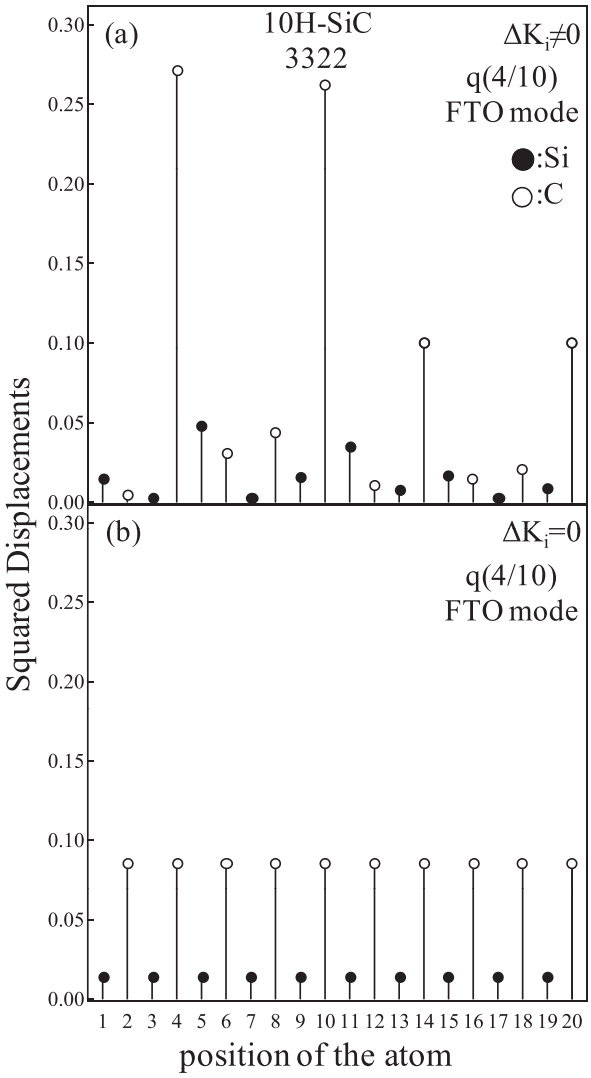

FIG. 7. Calculated displacement patterns of $q(4/10)$ mode (a) for $\Delta K \neq 0$ and (b) for $\Delta K = 0$; force-field parameters given in Table I are used in the calculation.

parameters ΔK_1 and ΔK_3. However, we did not examine the effect of these parameters in detail because the influence of ΔK_1 and ΔK_3 is small compared with that of ΔK_2. Figure 6 reveals that the relative intensity of $I(6/10)/I(4/10)$ varies strongly with ΔK_2, whereas $I(8/10)/I(4/10)$ varies weakly. The value of the observed intensity, $I(6/10)/I(4/10)$ is 0.45, the corresponding value of ΔK_2 is 0.235.

C. Atomic displacement patterns and ΔK

The calculated Raman intensity for the $q(6/10)$-folded mode of 10H-SiC depends strongly on the force-field difference ΔK_i between the cubic and hexagonal environments. The intensity of this mode is especially sensitive to the choice of the force constant $\Delta K_2 (= \Delta K_2^{cc})$, but insensitive to ΔK_1 $(= \Delta K_{-3}^{cs})$ and ΔK_3 $(= \Delta K_2^{ss})$ for the 10H polytype. We can fit the calculated Raman spectral profiles of 10H-SiC to the experimental data using the best-fit parameters listed in Table I. It should be noted that the set of force constants listed in Table I are useable as universal parameters for various polytypes other than 10H. These parameters deviate by a few

percent from the values employed in Ref. 2. Usually, force-field parameters are determined so that the calculated frequencies fit the experimental phonon frequencies. The present Raman intensity analysis demonstrates that the force-field parameters should be chosen under the condition that the calculated Raman intensity profiles are in accord with the experimental data. This constraint is more severe than the restriction relevant to the phonon frequencies, and the force-field parameters would be determined with higher accuracy.

We shall show that the atomic displacements patterns are strikingly changed by the introduction of force-field difference ΔK_i. The vibrational amplitudes of the Si and C atoms in 10H-SiC is calculated using the equations of motion (Eq. (2)) when ΔK_i is present or not. In Figs. 7(a) and 7(b), the atomic displacement patterns in the unit cell of 3322 are depicted for when ΔK_i does and does not exist, respectively.

In this calculation, we used the force constant values in Table II for the force-field differences. The atomic displacement pattern given by Fig. 7(a) provides the Raman intensity profiles fitted to the experimental profiles, whereas the atomic displacement given in Fig. 7(b) provides a relatively weak FTO mode intensity. As shown in Fig. 7(a), the distortion of the atomic displacement pattern induced by the force-field difference is pronounced for $\Delta K_i \neq 0$, whereas for $\Delta K_i = 0$, the displacement pattern is sinusoidal-like and a slow-varying function of position, as shown in Fig. 7(b). This deformation pattern in Fig. 7(a) contributes to the Raman intensity enhancement of the FTO modes in SiC polytypes. As is seen in Fig. 5, the noticeable intensity enhancement of the FTO modes is observed in 15R:$(32)_3$, 27R:$(3222)_3$, and 10H:(3322), whereas it is not appreciably obvious in 6H-SiC (33) and 8H-SiC(44), although these are not shown here. The Raman intensity enhancement induced by the force-field difference might be specific to the lower symmetry 32 stacking sequence. The existence of a force-field difference in the hexagonal and cubic envelopments in α-SiC provides an atomic displacement modified from 3C's displacement. This modified (distorted) displacement pattern breaks the cancelation of the bond Raman polarizabilities in a unit cell and results in an enhancement of the Raman intensity.

V. CONCLUSION

In the present work, the stacking structure of the 10H-SiC crystal has been determined from the fitting of the calculated Raman intensity profile to the experimental profile. The stacking sequence inferred by the Raman intensity analysis is 3322. Furthermore, the present Raman intensity analysis confirms the empirical rule that the reduced wavevector of the FTA and FTO modes having maximum intensity is equal to the hexagonality of the polytype crystal studied. A certain FTO band has relatively increased strength for 10H-SiC. These enhancements of the Raman intensity for the specified folded modes are derived from the peculiar force-field distributions in the higher-ordered SiC polytypes. The distortion of the displacement pattern arising from the force-field difference in the hexagonal and cubic environments would contribute to the enhancement of the Raman intensity of the specified folded modes.

[1]S. Nakashima, H. Katahama, Y. Nakakura, and M. Mitsuishi, Phys. Rev. B **33**, 5721 (1986).
[2]S. Nakashima and K. Tahara, Phys. Rev. B **40**, 6339 (1989).
[3]S. Nakashima, H. Harima, T. Tomita, and T. Suemoto, Phys. Rev. B **62**, 16605 (2000).
[4]S. Nakashima and H. Harima, Phys. Status Solidi A **162**, 39 (1997).
[5]D. W. Feldman, J. H. Parker, Jr., W. J. Choyke, and L. Patrick, Phys. Rev. **173**, 787 (1968).
[6]S. Nakashima, A. Wada, and Z. Inoue, J. Phys. Soc. Jpn. **56**, 3375 (1987).
[7]S. Nakashima, Y. Nakakura, and Z. Inoue, J. Phys. Soc. Jpn. **56**, 359 (1987).
[8]S. Nakashima, K. Kisoda, and J.-P. Gauthier, J. Appl. Phys. **75**, 5354 (1994).
[9]L. S. Ramsdell and J. A. Kohn, Acta Cryst. **4**, 111 (1951).
[10]D. Pandey and P. Krishna, Mater. Sci. Eng. **20**, 243 (1975).
[11]Z. Inoue, J. Mater. Sci. **17**, 3189 (1982).
[12]H. P. Iwata, U. Lindefelt, S. Öberg, and P. R. Briddon, Physica B **340–342**, 165 (2003).
[13]W. H. Backes, P. A. Bobbert, and W. van Haeringen, Phys. Rev. B **49**, 7564 (1994).
[14]S. Limpijumnong and W. Lambrecht, Phys. Rev. B **57**, 12017 (1998).
[15]K. Kobayashi and S. Komatsu, J. Phys. Soc. Jpn. **81**, 024714 (2012).
[16]S. Nakashima, H. Ohta, M. Hangyo, and B. Palosz, Philos. Mag. B **70**, 971 (1994).
[17]S. Nakashima, S. Katahama, Y. Nakakura, A. Mitsuishi, and B. Patosz, Phys. Rev. B **31**, 6531 (1985).
[18]S. Nakashima and M. Balkanski, Phys. Rev. B **34**, 5801 (1986).
[19]M. Wolkenstein, C. R. Acad. Sci. URSS **30**, 791 (1941).
[20]M. Eliashevitch and M. Wolkenstein, J. Phys. USSR **9**, 101 (1945); **9**, 326 (1945).
[21]D. A. Long, Proc. R. Soc. London, Ser. A **217**, 203 (1953).
[22]R. Tubino and L. Piseri, Phys. Rev. B **11**, 5145 (1975).
[23]S. Go, H. Bilz, and M. Cardona, Phys. Rev. Lett. **34**, 580 (1975).
[24]A. A. Maradudin and E. Burstein, Phys. Rev. **164**, 1081 (1967).
[25]S. Nakashima and K. Tahara, Phys. Rev. B **40**, 6345 (1989).
[26]S. Nakashima and M. Hangyo, Solid State Commun. **80**, 21 (1991).